International Journal of Engineering Research & Technology (IJERT)
ISSN: 2278-0181
Vol. 14 Issue 11 , November - 2025

Powerline Channel Modeling Approaches: A Comprehensive Survey

A. M. Nyete
Department of Electrical and Information Engineering
University of Nairobi

Abstract: Power line communication (PLC) offers a convenient and low cost way of transmitting data. But, this technology faces some serious challenges to do with the channel type and characteristics, and the noise in it. Numerous efforts have been made to model the channel behavior so as to understand the channel properties better. Given that the PLC network is designed for power delivery, understanding the channel properties is key in the design of a PLC system that can deliver high and reliable data rates. The modelling and understanding of the channel transfer function is very crucial as it affects the choice of the appropriate modulation and coding schemes; a key consideration in data communications. Even though several researchers have devoted their time in determining accurate channel models for the PLC, so far, there is no universally accepted model in the PLC community. In this paper, a comprehensive survey of the different PLC channel modelling approaches is presented, together with the associated PLC channel modelling challenges.

1 INTRODUCTION

Power lines are designed to carry electric power. However, the extensive coverage that the power lines have reached in recent years has attracted the attention of communication engineers who see it as the cheapest medium for modern day communications. This has led to the emergence of power line communications [PLC]; which essentially refers to the transfer of voice, data and video signals between the transmitter and the receiver over the electrical power network. PLC technology is primarily attractive because the power line network is already in place, which greatly brings down the cost of setting up a communications network. Hence, many research efforts have been fronted that are geared towards the investigation of the characteristics of the PLC channel. These efforts range from the study of the channel frequency response, attenuation, noise characteristics, multipath effects, throughput as well as coding and modulation options that best suit this channel [1-20]. A simplified diagram of a power line communication network is shown in Figure 1.

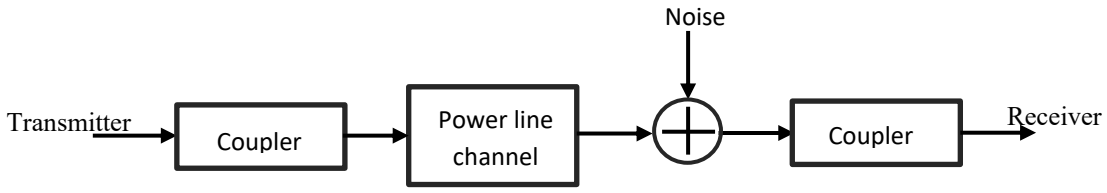

Figure 1: A simplified block diagram of a power line communication network

Currently, PLC applications can be categorized into two broad categories: the “last mile” and the “last inch” access. The “last mile” application in networking solutions refers to the use of the PLC channel in providing a communications link between the last point of connection at the distribution layer (may be the local distribution transformer) and the customer premises. Fig. 2 below shows an example of such an application. On the other hand, the “last inch” application refers to the use of PLC technology in providing networking communication channel inside the customer premises; see Fig. 3 for an illustration. PLC technology is not necessarily better than other communication technologies, neither are these other technologies without challenges of their own, or to put in other words; superior to PLC technology. However, PLC has a clear edge over the other technologies owing to the fact that a socket terminates at every room in every house that is connected to the power grid, thus providing readily available medium of

International Journal of Engineering Research & Technology (IJERT)
ISSN: 2278-0181
Vol. 14 Issue 11 , November - 2025

communication [1, 15]. The power line network is by far be the most expansive and ubiquitous in the world both at the core, distribution and access layers.

PLC technology is broadly divided into two categories depending on the frequency band and the data throughput rate. These are the narrowband and broadband PLC. Narrowband PLC (NB-PLC) operates in the frequency band 3-500 KHz while broadband PLC (BB-PLC) usually operates at frequencies between 1-300 MHz. Further, NB-PLC can be sub-classified into low data rate and high data rate applications. NB-PLC applications have a throughput that is limited to a few kbit/s and are also based on single carrier technology. This category of PLC system is mainly applied in automation of metering solutions, low data rate interconnections and control of home appliacnces through power sockets in every room, street lighting control, ground-lights control in airport runways, home automation and application in control data communication with 40 kbit/s in street car/subway systems on 750V direct current networks . BB-PLC data rates are in the megabit per second range. Broadband PLC networks are an ideal solution for advanced information technology applications such as high speed data transfer, real-time video streaming and high definition television (HDTV) as well as voice connections [1, 17-21].

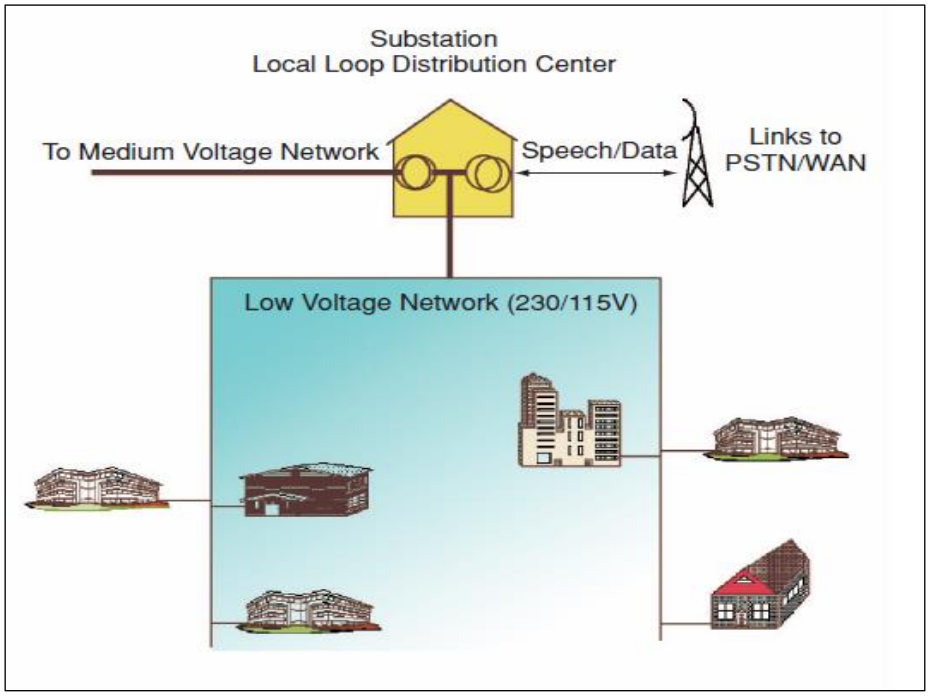

Figure 2: The “last mile” broadband connection to homes and offices from a local distribution center [16]

International Journal of Engineering Research & Technology (IJERT)
ISSN: 2278-0181
Vol. 14 Issue 11 , November - 2025

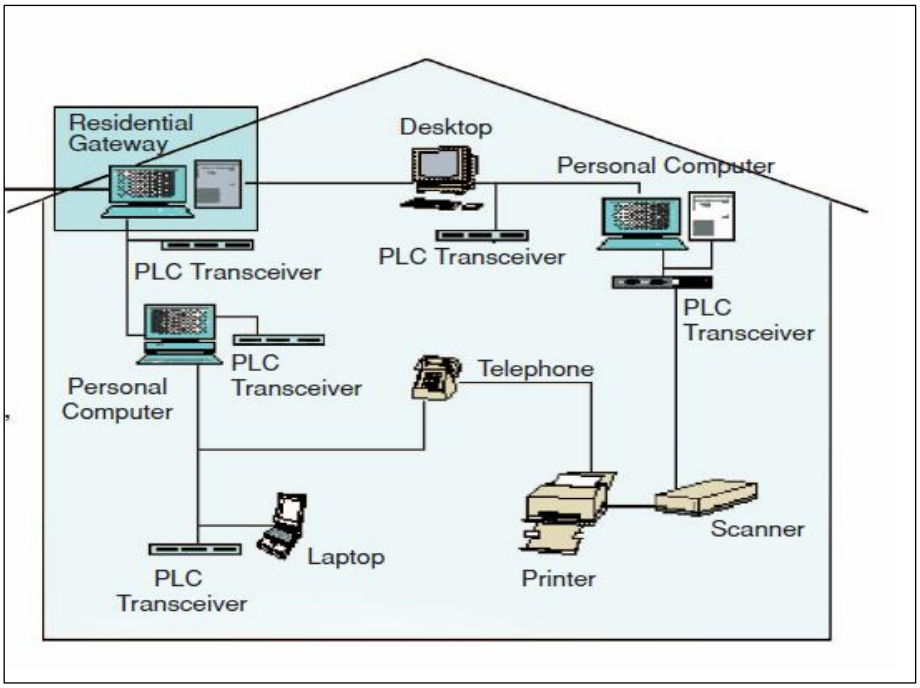

Figure 3: The "last-inch" access or in-house networking [16]

The fact that the power lines were designed with the primary goal of transmitting electrical power means that the channel is not that favorable for communication purposes. Thus the PLC channel is hostile in as far as communication needs are concerned. This is so because the channel is plagued by impedances that vary both with time and frequency, attenuation that is frequency dependent, multipath effects that arise from multiple branches and nodes, different noise types as well as electromagnetic compatibility issues that limit the transmit power [17,19]. Thus there is need to study and understand the channel behavior in different loading conditions and noise types. The studies would range from obtaining the channel transfer function, throughput analysis and modeling, noise measurements and modeling, and study of the channel response when different coding and modulation schemes are used to enhance the channel performance [6, 12, 15, 17-19, 22]. The channel performance can be measured in terms of the bit error rate (BER) and the signal to noise ratio (SNR).

However, the biggest problem in the characterization of the PLC channel properties would be to come up with a model that describes all the channel characteristics and incorporates all the measurements into a mathematical model, and still remains physically meaningful in terms of the distribution both in space and time, and also remains simple to the point that any required statistics can be extracted for solving any problem to do with signal transmission and reception. Thus the characterization of the PLC channel, like any other communication channel, is a tradeoff between system complexity and performance. All in all, there is no universally accepted channel and noise models for the PLC channel currently, and efforts to get some are an on-going exercise. Different researchers and academicians have proposed models of the PLC channel base on analytical derivations and/or from measurements.

Power line networks differ in terms of structure, topology and the physical properties from other transmission media such as coaxial cables, fiber-optic cables and twisted pair cables, and wireless channels, among other media. The power line environment is hostile when used for data and voice communication. The channel is very dynamic both in time and space, which means that the channel properties are hard to accurately predict and/or model. For practical purposes, models of the channel frequency response, channel availability and reliability as well as noise models are of interest. In contrast though, most of the models developed to define the above channel characteristics are very limited in terms of their practical value [1-6].

For the channel transfer characteristics (frequency response), most of the models are limited due to the fact that they are based on bottom-up approaches which means that the network behavior is described in terms of a large number of distributed components. Normally, such components are described in form of matrices which describe their properties, based on either scattering parameters or admittance and four-pole values [6, 22, 23]. This means that the details of all the network components, that is, cables, connected

International Journal of Engineering Research & Technology (IJERT)
ISSN: 2278-0181
Vol. 14 Issue 11 , November - 2025

devices and joints (nodes) are needed for the setting up of the above matrices. But, from a practical perspective, it would be impossible to determine all the parameters associated with each of these network elements with sufficient precision.

On the contrary, a more practical approach would be to measure the channel transfer function between the input and the output by assuming that the network is a black box. This approach is usually referred to as the top-down method. This approach is the one adopted in [4-6, 24]. In [24], an attenuation and noise model is presented based on measurements. This model is narrowband in that its frequency range is restricted to below 150 KHz. The model described in [6] describes the channel transfer characteristics in the range of frequencies between 500 KHz and 20 MHz; thus this model can be used for broadband applications. The model describes the channel multipath properties in very few relevant parameters, as compared to complexity associated with the bottom-up strategy. The channel parameters are derived from measurements. The basic idea in this approach were first explored in [4] and at the same time a less precise though simpler multipath model derived in [5].

Only in the simplest of cases, that is a single branch network, can the physical explanation for the measured results be identified in terms of the cable losses, transmission as well as reflection factors. In real networks, comprising of many branches and nodes, the back-tracing of the observed results to the physical nature of the network would be an impossible task. Thus the top-down methodology is a more realistic and simpler approach.

2 PLC CHANNEL MODELS

The power line channel is one of the most complex channels to describe in terms of the constituent elements in the network as described above. Thus, most of the models that are in existence today are based on the measured network response which is then related to particular known electric or electronic phenomena. Alternatively, the phenomena are used to predict the PLC channel response and then measurements are done to test how close the measurements and predictions come. Earlier models of the channel frequency response are the multipath model of Zimmermann and Dostert [4, 6], the echo model of Philipps [5], Meng *et al.* model [9], Anatory *et al.* model [7, 25] and the Esmaillian model [26], among others.

2.1 Zimmermann and Dostert Multipath Model

A typical power distribution network consists of numerous branches and nodes. If the power network is used as a communication channel, the signal is bound to suffer from multiple reflections and at the end of the day, it will undergo multipath propagation. The various nodes (interconnection points) within the network act as possible scattering/reflection points for the signal. Thus the signal travels back and forth before reaching the final destination. This is primarily so because the different branches that are interconnected from one node have different complex impedances. It is on this basis that Zimmermann and Dostert [4, 6] proposed a multipath model for the powerline channel.

If we consider the signal that travels through a complex power line network, it becomes rather obvious that there is no direct line of sight path between the transmitting and receiving antenna. Thus, different copies (echoes) of the signal that are attenuated and delayed in different proportions arrive at the receiving antenna. The kind of fading experienced in this case is frequency selective. The model was first developed by considering the simplest of a power network that can be; a single node network with one branch. This is illustrated in Fig. 4 below. The network consists of three elements (1), (2) and (3) with lengths L_1, L_2 and L_3 and the characteristic impedances Z_{L1}, Z_{L2} and Z_{L3} respectively. With the assumption that points A and C are matched, which makes $Z_A = Z_{L1}$ and $Z_C = Z_{L2}$, the reflection points are B and D, with the reflection coefficients r_{1B} , r_{3B}, r_{3D} and the transmission coefficients are t_{1B}, t_{3B}.

International Journal of Engineering Research & Technology (IJERT)
ISSN: 2278-0181
Vol. 14 Issue 11 , November - 2025

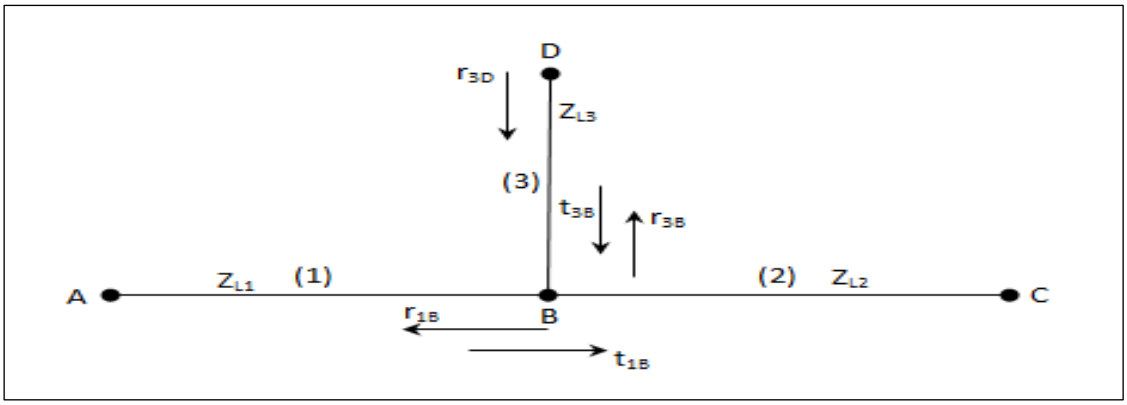

Figure 4: Multipath propagation: Cable with one tap [6].

With these assumptions in place, the link may have an infinite number of propagation paths. Each path i, has a weighting factor g_i which represents the product of the reflection and transmission coefficients along the particular path. In [27], Gotz *et al.* have shown that after a reasonable number of paths, typically between 5-50 paths, the weight factor becomes negligible and the model is computed with a finite number of paths. From complex channel transfer function measurements, the authors came up with the following expression for the channel frequency response as a multipath environment [6]:

$$H(f) = \sum_{i=1}^{N} g_i \cdot e^{-(a_0 + a_1 f^k)\cdot d_i} \cdot e^{-j2\pi f \tau_i} \tag{1}$$

Where, N is the number of propagation paths, $g_i$is the weighting factor, a_0 , a_1 and exponent k are the parameters that define the frequency-dependent attenuation, d_i is the path length, τ_i is the path delay given by the following expression:

$$\tau_i = \frac{d_i}{v_p} = \frac{d_i\sqrt{\varepsilon_r}}{c_0} \tag{2}$$

Where ε_r is the insulating material's dielectric constant, c_0 is the speed of light, d_i is the length of a path and v_p is the propagation speed. Thus we can see from (1) that the model is characterized by three different components; the weighting factor, the attenuation portion and the delay portion. The factor $e^{-(a_0 + a_1 f^k)\cdot d_i}$ determines the amount of attenuation that takes place during signal transmission in the PLC channel. The factor $e^{-j2\pi f \tau_i}$ is the delay portion. The transmission and reflection coefficients are always less than one, and so, it goes without saying that the net product of all the transmission and reflection coefficients is also less than one, viz a viz:

$$|g_i| \leq 1 \tag{3}$$

The attenuation factor is obtained from the complex propagation constant by using transmission line analogy, that is:

$$\gamma = k_1\sqrt{f} + k_2 f + jk_3 f \tag{4}$$

Where $k_1\sqrt{f} + k_2 f$ is the attenuation constant and $k_3 f$ is the phase constant.

The constants k_1, k_2 and k_3 summarize the geometrical and material properties of the network. Thus it can be seen from (4) that the attenuation increases with frequency. The weighting and the delay factors are obtained when the frequency response of the PLC channel is converted into time domain. The weighting factor is inversely proportional to

International Journal of Engineering Research & Technology (IJERT)
ISSN: 2278-0181
Vol. 14 Issue 11 , November - 2025

the delay factor. This is due to the reduction in signal power as the signal travels through different points of discontinuity. This is depicted in Fig. 5 below. For the single branch network, reflection coefficients are obtained from:

$$r_{1b} = \frac{Z_{L2}||Z_{L3} - Z_{L1}}{Z_{L2}||Z_{L3} + Z_{L1}} \tag{5}$$

$$r_{3d} = \frac{Z_0 - Z_{L3}}{Z_0 + Z_{L3}} \tag{6}$$

$$r_{3b} = \frac{Z_{L2}||Z_{L1} - Z_{L3}}{Z_{L2}||Z_{L1} + Z_{L3}} \tag{7}$$

Where Z_0 is the characteristic impedance,.

Consequently, the transmission coefficients are obtained from:

$$t_{1b} = 1 - |r_{1b}| \tag{8}$$

$$t_{3b} = 1 - |r_{3b}| \tag{9}$$

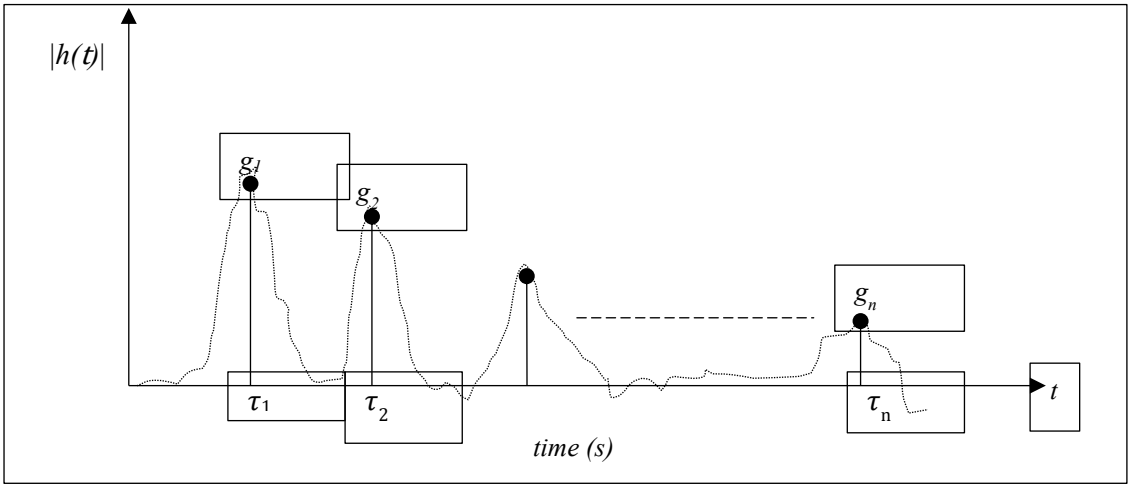

Figure 5: The impulse response of a single branch topology

However, it is noted that the complexity of this approach increases as the number of branches and nodes increases. Table1 summarizes the expressions for obtaining the three components of the Zimmermann and Dostert model for **N** paths.

International Journal of Engineering Research & Technology (IJERT)
ISSN: 2278-0181
Vol. 14 Issue 11 , November - 2025

Table 1: Model parameters for an N-path network [4]

path no.	signal direction	path length (d_i)	weighting factor (g_i)
1	$A \rightarrow B \rightarrow C$	l_1+l_2	t_{1b}
2	$A \rightarrow B \rightarrow D \rightarrow B \rightarrow C$	$l_1+2l_3+l_2$	$t_{1b} \times r_{3d} \times t_{3b}$
3	…	…	…
N	$A \rightarrow B \rightarrow (D \rightarrow B)^{N-1} \rightarrow C$	$l_1+2(N-1)\cdot l_3+l_2$	$t_{1b} \times r_{3d} \times (r_{3d} \times r_{3d})^{N-2} t_{3b}$

2.2 Philipps' models

The impedance characteristics of a PLC channel is highly variable with frequency and ranges between a few ohms to a few kilo ohms. The characteristics display the presence of both peaks and notches. At the peaks, the channel behaves like a parallel resonant circuit. In much of the frequency band, the impedance is either inductive or capacitive. The characteristic impedance of a powerline cable is around 90 Ohms. However, the net impedance in the network is determined by the topology of the network as well as the loads that are connected to it, whose impedances may be highly dependable on the frequency as well. Phillips also noted that the signal that is sent through the PLC channel will undergo reflections at points of impedance discontinuities and as a result echoes of the transmitted signal are produced. Thus, the powerline is regarded as an environment where multipath effects are prominent. This tallies with the views of Zimmerman and Dostert [4, 6].

Based on these observations concerning the powerline channel behavior, from extensive measurements by Philipps [28], two models were proposed for the PLC channel transfer characteristics; the echo model and the series resonant circuit model [5].

2.2.1 Echo model

The echo model is based on the multipath nature of the PLC channel which leads to direct as well as indirect transmission of the signal. Thus, the signal that gets to the receiver is a summation of several copies (echoes) of the transmitted signal, and not just one direct signal from the transmitter to the receiver. This means that different signals are delayed and attenuated differently. This fact led to the development of the echo model, which happens to be in good agreement with the parameters that constitute the network.

If we assume that there are N paths that the signal travels through to the receiver, then, on the path v, the signal will suffer the amount of delay equal to τ_v and also be attenuated by a complex factor ρ_v. The complex path attenuation is given by [5]:

$$\rho_v = |\rho_v| \cdot e^{-j\varphi_v} \tag{10}$$

where:

$$\varphi_v = tan^{-1}\left(\frac{Im(\rho_v)}{Re(\rho_v)}\right) \tag{11}$$

Then, the impulse response $h(t)$ is obtained as a sum of N dirac pulses which are multiplied by ρ_v and delayed by τ_v, that is:

$$h(t) = \sum_{v=1}^{N} |\rho_v| \cdot \delta(t - \tau_v) \tag{12}$$

International Journal of Engineering Research & Technology (IJERT)
ISSN: 2278-0181
Vol. 14 Issue 11 , November - 2025

The channel transfer function is obtained as a Fourier transform of the impulse response, from which we have:

$$H(f) = \sum_{v=1}^{N} |\rho_v| . e^{j\varphi_v} \cdot e^{-j2\pi f \tau_v} \quad (13)$$

The graphical representation of the echo model is shown in Fig. 6. For each path, there are three parameters that have to be defined. Hence, for a model with N paths, a total of $3N$ parameters will be required to completely define the model. These parameters are the delay factor τ_v, the phase shift φ_v and the attenuation factor ρ_v. The said model can be optimized by using an evolutionary strategy as described in [5] which essentially minimizes the root mean square error and maximizes the correlation factor between the measured and modeled functions.

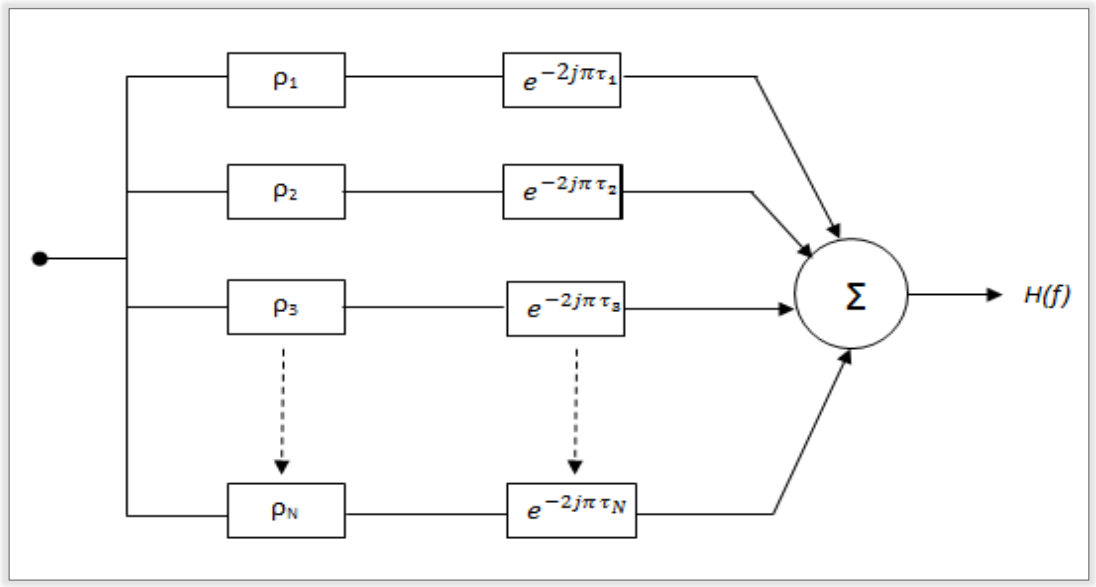

Figure 6: Graphical representation of the Echo model

2.2.2 Series *resonant circuit model*

Electrical load impedance measurements have been shown to behave like one or few series resonant circuits whose constituent elements are a resistance R, inductance L and a capacitance C. This is due to the fact that many appliances incorporate a capacitance at the input for preventing interference and also possess a feeder line that is both resistive and inductive. Since in most cases the loads are very much far apart, they do not influence one another. Hence it would be realistic to model the powerline channel as a cascade of series resonant circuits (SRC) that are decoupled. Fig 7 below shows a single RLC resonant circuit connected to line of a load impedance Z.

International Journal of Engineering Research & Technology (IJERT)
ISSN: 2278-0181
Vol. 14 Issue 11 , November - 2025

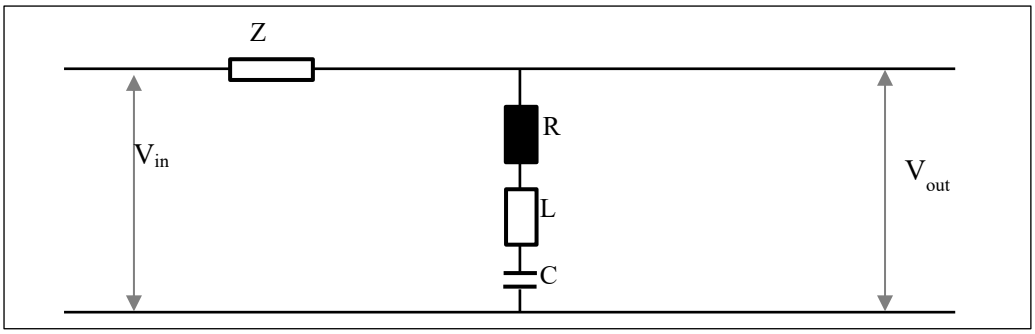

Figure 7: Series RLC resonant circuit

The frequency-dependent impedance of the series RLC resonant circuit is calculated as :

$$Z_S = R + j \cdot 2\pi f \cdot L + \frac{1}{j \cdot 2\pi f \cdot C} \tag{14}$$

At resonance, the capacitive and inductive reactances are equal, and the circuit is purely resistive (minimum impedance). The resonant frequency is then computed from:

$$f_{res} = \frac{1}{2\pi\sqrt{L.C}} \tag{15}$$

Then, the channel frequency response is given by:

$$H(f) = \frac{1}{1 + \frac{Z}{Z_S(f)}} \tag{16}$$

The channel frequency response is shown in the Fig. 8 below; where we see that a notch occurs in the amplitude transfer function at resonance.

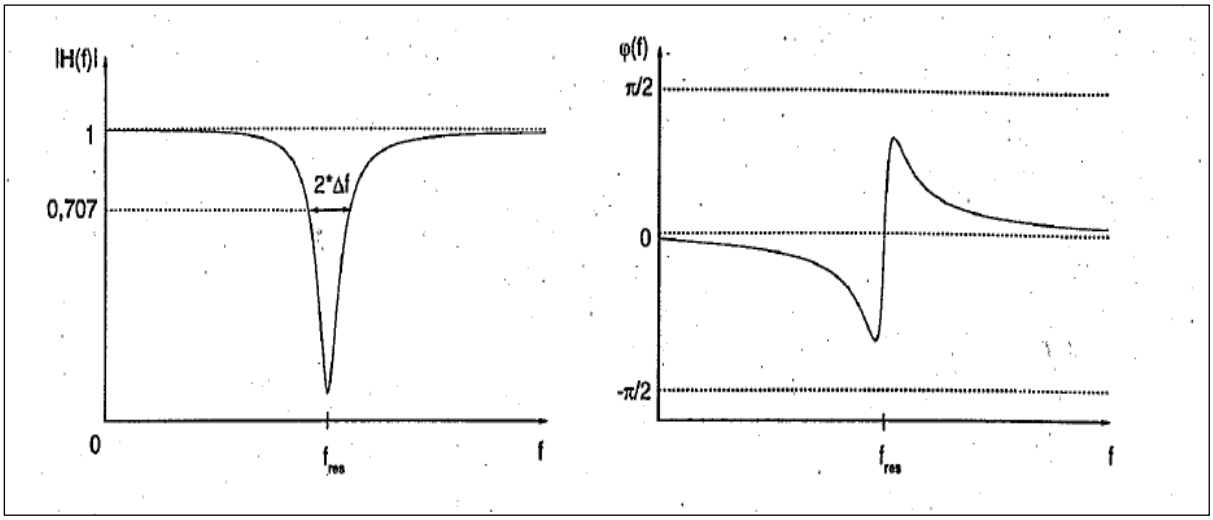

(a) Amplitude response (b) Phase response

Figure 8: The amplitude and phase response of a series RLC Circuit [5]

International Journal of Engineering Research & Technology (IJERT)
ISSN: 2278-0181
Vol. 14 Issue 11 , November - 2025

The quality factor (Q factor) of the circuit is given by:

$$Q = \frac{f_{res}}{2.\Delta f} = \frac{1}{R}\sqrt{\frac{L}{C}} \tag{17}$$

The quality factor is a function of the notch width; the narrower the notch, the higher the quality factor. In the phase response, we see that there is a steep rise at resonance. The phase is capacitive at lower frequencies while it is inductive at higher frequencies. The overall frequency response characteristic is modeled as a series of cascaded decoupled series resonant circuits, and is given by:

$$H(f) = \prod_{i=1}^{n} H_i(f) \tag{18}$$

In order to fit the model, 3*N* parameters should be optimized. The same approach adopted for the echo model can be used for the optimization. Table 2 shows the parameters that were obtained for a maximum of five series resonant circuits; that have been determined by using the evolutionary strategy.

Table 2 : Set of parameters of series resonance circuits model

No	R (Ohm)	L (μH)	C(nF)	f_{res} (MHz)	Q
1	21.4	0.137	10.8908	4.122	0.165
2	12.1	8.264	0.1334	4.793	20.640
3	67.9	18.919	0.0197	8.238	14.431
4	46.4	11.948	0.0103	14.324	23.183
5	19.6	1.008	0.0273	30.357	9.799

The frequency response of this kind of circuit is shown below in Figure 9 below.

International Journal of Engineering Research & Technology (IJERT)
ISSN: 2278-0181
Vol. 14 Issue 11 , November - 2025

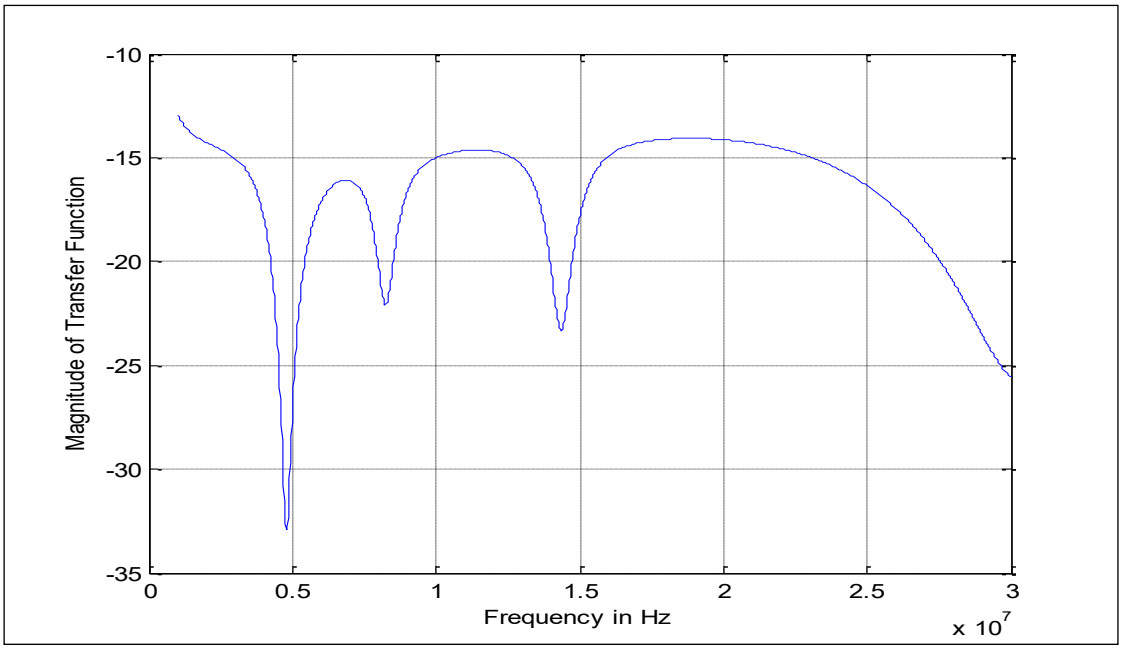

Figure 9: Channel transfer characteristic for a five series resonant circuits model

2.3 Meng et al. model

Meng *et al.* [9] applied transmission line theory to come up with a transfer characteristic model of the power line for a low voltage network. To validate the model, a sample network comprising of several branches and connected to different household appliances was constructed and the channel measurements were done. A simplified in-house powerline network with *N* branches is shown in Fig. 10 below.

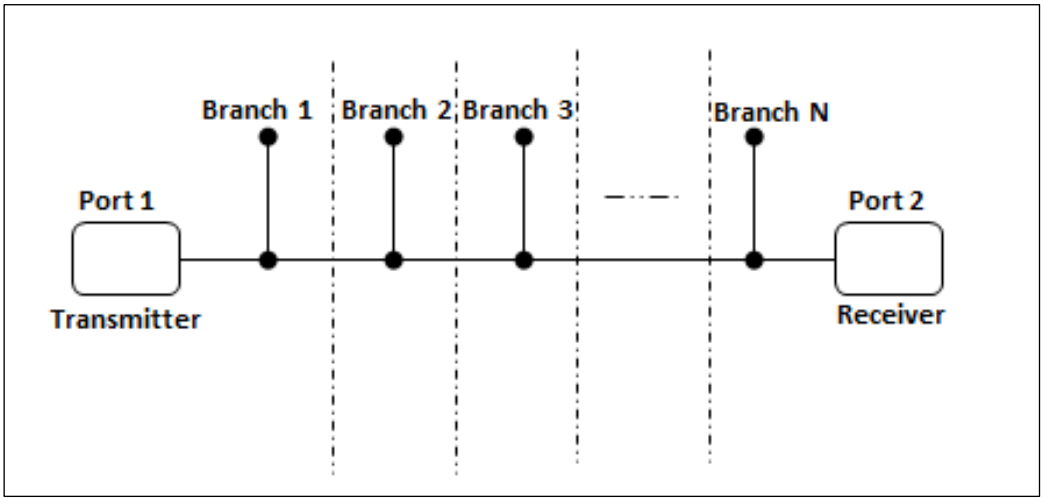

Figure 10: A simplified in-house powerline network with *N* branches

Four key parameters for the line are determined first, that is, the line resistance R, the line inductance L, the line capacitance C and the line conductance G. These primary parameters are necessary in the determination of the two model parameters; the propagation constant γ and the characteristic impedance Z_o. The mathematical procedure for the primary line parameter determination is a outlined below for each element:

International Journal of Engineering Research & Technology (IJERT)
ISSN: 2278-0181
Vol. 14 Issue 11 , November - 2025

1. RESISTANCE

Due to skin effect, when there is an ac current flow in the conductor, where more current flows near the conductor surface as opposed to towards the center. This is caused by the self-inductance within the conductor [9, 29]. This phenomenon causes an increase in the cable resistance which even becomes worse as the frequency of the current increases. Even though there is uniform current distribution throughout the cable cross section, when computing the cable resistance, it is normal to make the assumption that all the current flows within the cable "skin depth". The skin depth δ is computed as [9, 30]:

$$\delta = \sqrt{\frac{1}{\pi f \mu_c \sigma_c}} \tag{19}$$

Where μ_c is the permeability of the conductor, σ_c is the conductivity of the conductor, and f is the current frequency. Hence, for a transmission line consisting of two wires with a solid core conductor, its resistance is computed as:

$$R_{solid} = \frac{1}{\pi a \delta \sigma_c} \left(\frac{Ohms}{m}\right) \tag{20}$$

Where a is the conductor radius. If however the conducting wires are stranded, then the current flow area is reduced due to the gaps between the wire strands. In such cases, the solid cable resistance is multiplied with a correction factor. This correction factor is given by [9]:

$$X_R = \left[Cos^{-1}\left(\frac{r_{wire}-\delta}{r_{wire}}\right) \times {r_{wire}}^2 - (r_{wire}-\delta) \times \sqrt{{r_{wire}}^2 - (r_{wire}-\delta)^2}\right] / (2 \times (r_{wire} \times \delta) \tag{21}$$

Where r_{wire} is the a single wire strand radius, and δ is as defined in (19) above. Thus, the net resistance of the stranded conductor is given by [9]:

$$R = X_R \times R_{solid} \left(\frac{Ohms}{m}\right) \tag{22}$$

2. INDUCTANCE

For a transmission line comprising of two wires, its net inductance is a summation of the self-inductance per conductor and the mutual inductance between them. The self-inductance L_s is calculated as follows [29]:

$$L_s = \frac{\mu_c}{8\pi} \quad \left(\frac{H}{m}\right) \tag{23}$$

Also, the mutual inductance is computed using the following expression [29]:

$$L_m = \frac{\mu_c}{\pi} In\left(\frac{D-a}{a}\right) \quad \left(\frac{H}{m}\right) \tag{24}$$

Where D is the distance between the conductors. So, the net inductance is given as [29]:

$$L = L_s + 2L_m = \frac{\mu_c}{\pi}\left[\frac{1}{4} + In\left(\frac{D-a}{a}\right)\right] \left(\frac{H}{m}\right) \tag{25}$$

International Journal of Engineering Research & Technology (IJERT)
ISSN: 2278-0181
Vol. 14 Issue 11 , November - 2025

3. CAPACITANCE

The two-wire cable capacitance is a function of the cable to cable capacitance per unit length, C_{cable}, and the capacitance due to the coupling effects from both the metal conduit, $C_{conduit}$ and the earth cable. The capacitance between the metal conduit and the earth cable is zero because both of them are grounded which means that the potential between them is zero also. The cable capacitance per unit length, C_{cable} is given by [29]:

$$C_{cable} = \frac{\pi\varepsilon}{In[\left(\frac{D}{2a}\right) + \sqrt{(\frac{D}{2a})^2 - 1}]} \quad \left(F/m\right) \tag{26}$$

Where ε is the dielectric material permittivity between the conductors. The capacitance due to the coupling effects from the metal conduit, $C_{conduit}$, is given by [9]:

$$C_{conduit} = \lim_{N\to\infty} \sum_{k=1}^{N} \frac{1}{N} \times \frac{2\pi\varepsilon_k}{In(\frac{b_k}{a})} \quad \left(F/m\right) \tag{27}$$

Where ε_k and b_k are dielectric material permittivity and the metal conduit inner radius for the sector *k*. The net capacitance, *C* is then obtained from [9]:

$$C = C_{cable} + \frac{C_{cable}}{2} + \frac{C_{conduit}}{2} = \frac{3C_{cable}}{2} + \frac{C_{conduit}}{2} \left(F/m\right) \tag{28}$$

4. CONDUCTANCE

From [29], we see that if the medium is homogeneous, then the following expression holds true:

$$\frac{C}{G} = \frac{\varepsilon}{\sigma} \tag{29}$$

which implies that,

$$G = \frac{\sigma C}{\varepsilon} \tag{30}$$

Where σ is the dielectic material conductivity and G is the cable conductance per unit length. In the approach taken by Meng *et al.*, the dielectric material is assumed to be a mixed content and the space inhomogeinity is neglected to make the model more tractable.

Based on the lumped-element circuit model of the transmission line, the propagation constant γ and the characteristic impedance Z_o can be computed as [9, 29]:

$$\gamma = \alpha + j\beta = \sqrt{(R + j\omega L)(G + j\omega C)} \tag{31}$$

$$Z_o = \sqrt{\frac{R + j\omega L}{G + j\omega C}} \tag{32}$$

International Journal of Engineering Research & Technology (IJERT)
ISSN: 2278-0181
Vol. 14 Issue 11 , November - 2025

Where ω is the angular frequency. The real part of the propagation constant α is the attenuation constant while the imaginary part is the phase constant β. Thus we see that these parameters can be used to characterize any transmission line regardless of its length. The input impedance Z_{in} of a transmission line whose length is l and is terminated by a load impedance Z_L is given by:

$$Z_{in} = Z_o \frac{Z_L + Z_o \tanh(\gamma . l)}{Z_o + Z_L \tanh(\gamma . l)} \ (Ohms) \tag{33}$$

If the load is a short circuit, then $Z_L = 0$, which gives:

$$Z_{is} = Z_o \tanh(\gamma . l) \ \ (Ohms) \tag{34}$$

If however the load impedance is replaced by an open circuit, then $Z_L = \infty$, and we have:

$$Z_{io} = Z_o \coth(\gamma . l) \ \ (Ohms) \tag{35}$$

From the Equations (34) and (35), we can obtain the characteristic impedance and the propagation constant as follows:

$$Z_o = \sqrt{Z_{is} Z_{io}} \tag{36}$$

$$\gamma = tanh^{-1} \sqrt{\frac{Z_{is}}{Z_{io}}} \tag{37}$$

The diagram shown in Fig. 11 is used for the s-parameters evaluation for a single-branch network. In the derivation that follows, the path line is defined as the direct path for the signal (excluding the branches). Line 1 is the path power line with line parameter Z_o, γ, Line 2 is the branch power line with line parameter Z_o, γ, Line 3 is the transmission line with 50Ω characteristic impedance. By applying the theory of the transmission line, Z_{in1}, Z_{in2}, Z_{in}, Γ_1 and Γ_2 are determined as follows [9]:

$$Z_{in1} = Z_o \frac{Z_L + Z_o \tanh(\gamma . l_3)}{Z_o + Z_L \tanh(\gamma . l_3)} \ (Ohms) \tag{38}$$

$$Z_{in2} = Z'_o \frac{Z_b + Z'_o \tanh(\gamma . l_2)}{Z'_o + Z_b \tanh(\gamma . l_2)} \ (Ohms) \tag{39}$$

$$Z_{in} = Z_o \frac{(Z_{in1} // Z_{in2}) + Z_o \tanh(\gamma . l_1)}{Z_o + (Z_{in1} // Z_{in2}) \tanh(\gamma . l_1)} \ (Ohms) \tag{40}$$

International Journal of Engineering Research & Technology (IJERT)
ISSN: 2278-0181
Vol. 14 Issue 11 , November - 2025

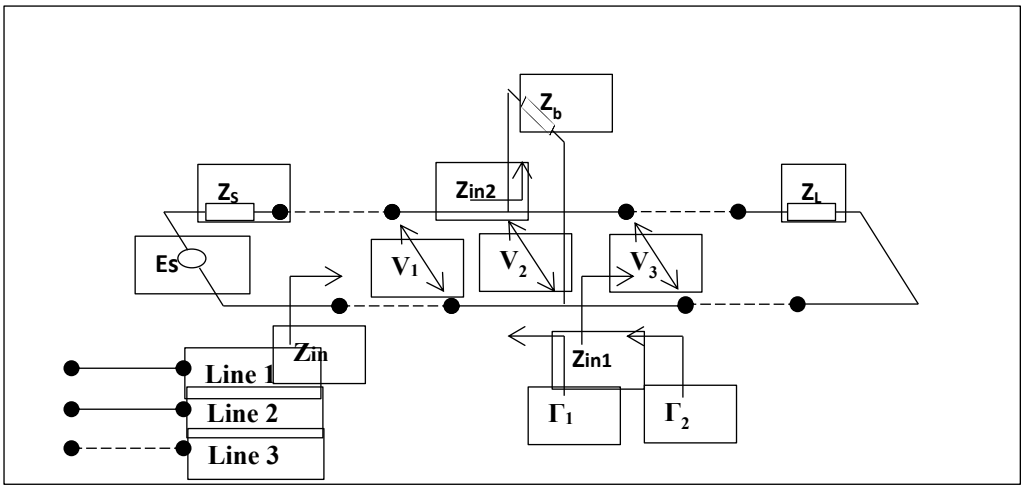

Figure 11: Single-branch network diagram

Where Z_s is the source impedance, Z_L is the load impedance, Z_b is the load impedance at the branch end, Z_{in1} is the input impedance of the network on the right of the tap, Z_{in2} is the input impedance of the branch network, Z_{in} is the input impedance of the single branch network, Γ_1 is the reflection coefficient from path end, and Γ_2 is the reflection coefficient from tap point calculated as:

$$\Gamma_1 = \frac{Z_L - Z_0}{Z_L + Z_0} \tag{41}$$

And,

$$\Gamma_2 = \frac{Z_{in1}||Z_{in2} - Z_0}{Z_{in1}||Z_{in2} + Z_0} \tag{42}$$

The s-parameters S_{11} and S_{21} are obtained using the following equations [31]:

$$S_{11} = \frac{Z_{in} - 50}{Z_{in} + 50} \tag{43}$$

$$S_{21} = 2\,\frac{V_3}{E_g} \tag{44}$$

The S_{21} parameter can also be calculated indirectly according to the following equation:

$$S_{21} = 2\,\frac{V_3}{V_2}\cdot\frac{V_2}{V_1}\cdot\frac{V_1}{E_g} \tag{45}$$

Where,

$$\frac{V_1}{E_{g_1}} = \frac{Z_{in}}{Z_{in} + Z_g} \tag{46}$$

From [30], the shifting of reference planes yields the following:

International Journal of Engineering Research & Technology (IJERT)
ISSN: 2278-0181
Vol. 14 Issue 11 , November - 2025

$$\frac{V_3}{V_2} = \frac{(1+\Gamma_1)\, e^{-\gamma l_3}}{1+\Gamma_1 e^{-\gamma l_3}} \tag{47}$$

$$\frac{V_2}{V_1} = \frac{(1+\Gamma_2)\, e^{-\gamma l_1}}{1+\Gamma_2 e^{-\gamma l_1}} \tag{48}$$

After determining the S-parameters above, we can then obtain the scattering matrix for an entire network comprising several cascaded single branch networks. There are two methods that can be applied to do this. One is the use of signal flow graphs while the other one is the use of the chain scattering matrix (T-matrix). For ease of computation, the latter is used in this case. The overall T-matrix for the whole cascaded network is a product of the individual T-matrices for each single branch network. The following is the relationship between the S-matrix and the T-matrix [9]:

$$[T] = \begin{bmatrix} \frac{1}{S_{21}} & -\frac{S_{22}}{S_{21}} \\ \frac{S_{11}}{S_{21}} & S_{12} - \frac{S_{11}S_{22}}{S_{21}} \end{bmatrix} \tag{49}$$

And then the total T-matrix for an entire network is calculated as [9]:

$$[T] = \prod_{k=1}^{N} [T_k] \tag{50}$$

Where T_k is the T-matrix of the k^{th} cascaded element in network. The S-matrix for the whole network can then computed as [9]:

$$[S] = \begin{bmatrix} \frac{T_{21}}{T_{11}} & T_{22} - \frac{T_{21}T_{12}}{T_{11}} \\ \frac{1}{T_{11}} & -\frac{T_{12}}{T_{11}} \end{bmatrix} \tag{51}$$

The S_{21} term gives the transfer function of the network.

2.4 Anatory et al. Model

The Anatory *et al.* model [7, 25] is based on the fact that at a particular node, part of the signal will be transmitted and another part will be reflected. The model also takes into consideration the loads connected to the network, their distances from the path line and the number of nodes. For a multiple branch transmission line at a single node as shown in Fig. 12, where Z_S is the impedance of the source, Z_n is the characteristic impedance of any terminal , and V_S and Z_L are source voltage and load impedance respectively, Anatory *et al.* developed the following transfer function for the PLC channel [7, 25, 32, 33]:

$$H_m(f) = \sum_{M=1}^{L} \sum_{n=1}^{N_T} T_{LM} \alpha_{mn} H_{mn}(f) \qquad n \neq m \tag{52}$$

International Journal of Engineering Research & Technology (IJERT)
ISSN: 2278-0181
Vol. 14 Issue 11 , November - 2025

Where: N_T, is the total number of branches connected at node B and terminated in any arbitrary load, n is any branch number, m is any referenced (terminated) load, M is the number of reflections (with a total L number of reflections),

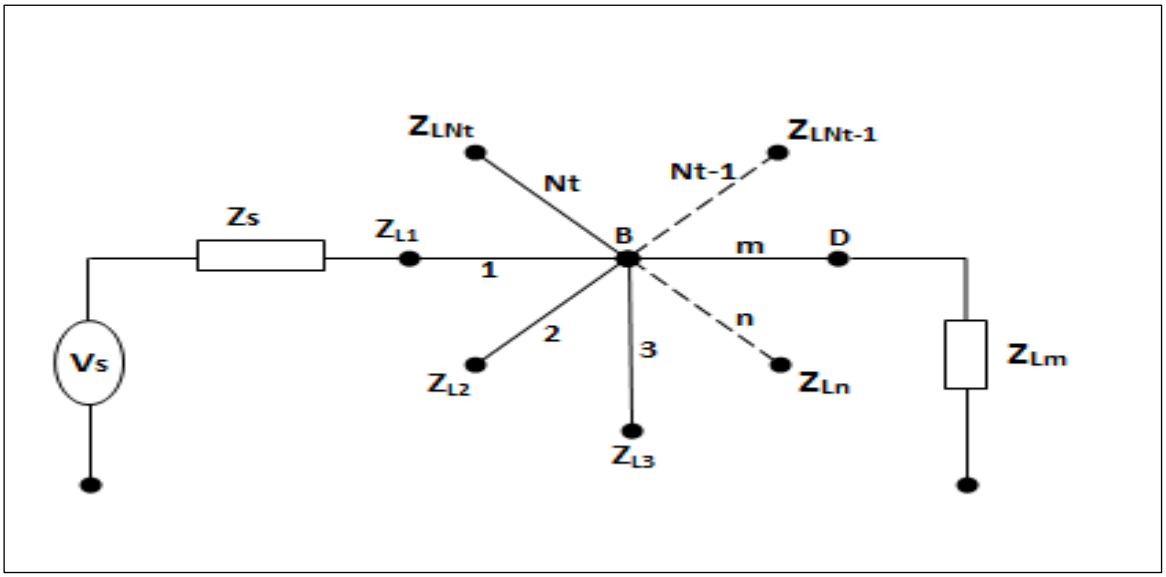

Figure 12: Single node power line network with multiple branches [32]

H_{mn} *(f)* is the transfer function between line n and a referenced load m, and T_{LM} is the transmission factor at the referenced load m, respectively. α_{mn} is the signal contribution factor given by:

$$\alpha_{mn} = P_{Ln}^{M-1} \rho_{nm}^{M-1} e^{-\gamma_n (2(M-1) l_n)} \tag{53}$$

Where ρ_{mn} is the the reflection factor at node B between line n and the referenced load m, and γ_n is the propagation constant of line n that has line length L_n. All terminal reflection factors P_{Ln} in general are given by:

$$P_{Ln} = \begin{cases} \rho_s & n = 1(source) \\ \rho_{Ln}, & otherwise \end{cases} \tag{54}$$

except at the source where $\rho_{L1} = \rho_S$ is the source reflection factor. The authors extended the above results for any power line network with spread branches as shown in Fig. 13.

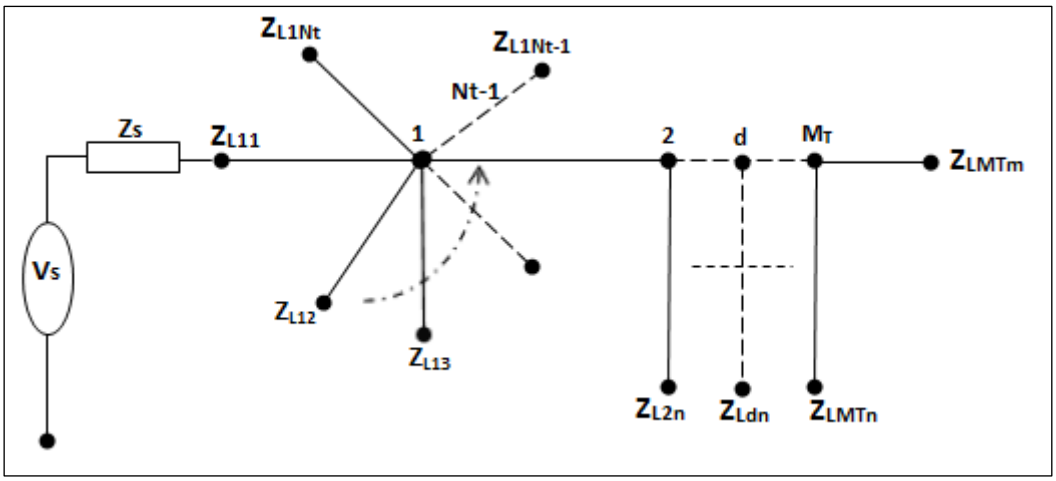

Figure 13: Power-line network with distributed branches

International Journal of Engineering Research & Technology (IJERT)
ISSN: 2278-0181
Vol. 14 Issue 11 , November - 2025

They obtained the transfer function of such a network as:

$$H_{mM_T}(f) = \sum_{d=1}^{M_T} \sum_{M=1}^{L} \sum_{n=1}^{N_T} T_{LM} \alpha_{mnd} H_{mnd}(f) \qquad n \neq m \tag{55}$$

$$\alpha_{mnd} = P_{Lnd}^{M-1} \rho_{nmd}^{M-1} e^{-\gamma_{nd}(2(M-1)l_{nd})} \tag{56}$$

$$P_{Lnd} = \begin{cases} \rho_s & d = n = 1(source) \\ \rho_{Lnd}, & otherwise \end{cases} \tag{57}$$

Where all the parameters used have the same significance as mentioned above and, M_T is the total number of distributed nodes, d is any referenced node (1… M_T), and $H_{mnd}(f)$ is the transfer function from line n to a referenced load m at a referenced node d.

2.5 Mulangu and Afullo model

Recently Mulangu and Afullo [34], investigated the effect of the number of branching nodes in a power line network and derived a PLC channel model that is based on Mie scattering theory [35]. The basis of this model is on the assumption of a multitude of scatterers that are randomly spread in the channel vicinity, requiring a sufficient number of impedance discontinuity points. The power line is considered as one single element, and then it is subdivided into a grid of scattering points (small areas) whose dimensions range from 0.5 to 3 mm. A power law mathematical formulation that relates specific attenuation in the channel to the number of branching nodes is then derived.

If an electromagnetic wave of known amplitude travels through a volume, containing N scattering particles that are identical with diameter D, its amplitude decreases by the factor of $e^{-\gamma l}$, at any distance l. The coefficient of attenuation γ is calculated as [34]:

$$\gamma = NQ_{ext}(D) \tag{58}$$

The wave attenuation in dB is then given by:

$$A_{dB} = 10 \log \frac{1}{e^{-\gamma l}} = 4.343 \gamma l \tag{59}$$

While the specific attenuation in dB/km computed as:

$$A_s = 4.343 \gamma \tag{60}$$

$$A_s[dB/km] = 4.343 \times 10^3 \int_0^{\infty} N(D) Q_{ext}(D) dD \tag{61}$$

Equation (61) can also be rewritten as:

International Journal of Engineering Research & Technology (IJERT)
ISSN: 2278-0181
Vol. 14 Issue 11 , November - 2025

$$A_s[dB/km] = 0.25\pi \int_0^{\infty} D^2 N(D) Q_{ext}(D) dD \quad (62)$$

The power law form of the specific attenuation is given as:

$$A_s = \varrho K^{\xi} \quad (63)$$

where ϱ and ξ are powerline specific coefficients and K is the branching nodes number.

2.6 Zwane and Afullo model

A series of resonant circuits (SRCs) can be used to describe the power line channel [5]. From channel measurements, a correlation of the notch locations to the SRC branch parameters was obtained. The transmission line theory for two extreme cases, that is, short circuited and open circuited branches, was used. Through the analysis of the input impedance characteristics around a resonant wavelength λ_r, the short and open circuited circuits behaved like a series RLC circuit. For the open circuited end, the cable length is in odd multiples of $\lambda_r/4$ while for the short circuited end, the cable length is in even multiples of $\lambda_r/2$. Table 3 presents a summary of the series RLC parameters determination formulations obtained.

Table 2: Series resonance RLC parameters [36]

Resonance	**Quarter wavelength ($\lambda_r/4$)** **Open circuit**	**Half wavelength ($\lambda_r/2$)** **Short circuit**
R	$\frac{1}{4} Z_0 \alpha \lambda_r$	$\frac{1}{2} Z_0 \alpha \lambda_r$
L	$\frac{\pi Z_0}{4 \cdot \omega_0}$	$\frac{\pi Z_0}{2 \cdot \omega_0}$
C	$\frac{4}{\pi \omega_0 Z_0}$	$\frac{2}{\pi \omega_0 Z_0}$
Q	$\frac{\beta_r}{2\alpha}$	$\frac{\beta_r}{2\alpha}$

Where in the above table, Z_0 is the characteristic impedance of the line, ω_0 is the resonant angular frequency, α is the attenuation constant of the line, λ_r is the wavelength at resonance and $\beta_r = \pi/l$. From Equation (2.16), each resonant circuit is described by a transfer function $Hr_i(f)$ and the overall transfer function is given as:

$$H(f) = A \prod_{i=1}^{n} Hr_i(f) \quad (64)$$

Where n is the number of series resonant circuits forming the total transfer function and A is the average path loss factor from transmitter to receiver distance determined by $e^{-\gamma d}$.

International Journal of Engineering Research & Technology (IJERT)
ISSN: 2278-0181
Vol. 14 Issue 11 , November - 2025

3. PLC CHANNEL MODELLING AND CHALLENGES

Even though the powerline channel and wireless channel have similarities, the PLC channel exhibits frequency selective fading with certain extent deterministic fact, quasi-static channel but with slow time variation and two-dimension attenuation characteristics. Therefore, it is challenging to model a realistic PLC channel. For the PLC channel transfer function, several approaches have been proposed in the last few years. The PLC channel modelling approaches cab be categorized into: the multipath approach and the transmission line approach or top-down and bottom-up techniques. For the multipath PLC channel, the most important task is to determine the number of paths and magnitude and delay of each path. Currently, the multipath models are based on the data obtained through field measurements on a powerline network. Hence, the channel responses can only be generated for limited scenarios by the multipath approach. For However, more flexibility can be obtained using the transmission line modelling approach. Through transmission line theory, the topology of the communication channel can be broken down into small units. For each unit, we can then determine the transfer function separately, and then, the entire PLC channel transfer function can be obtained by computed using the transmission line theory Chain Rule (CR) [35].

Essentially, the transmission line method can be used to determine the PLC channel response for a given random topology. However, the challenge is that it is cumbersome to achieve a unified calculation process for various topologies. Hence, if the transmission line method is used, the design process for each topology should be done manually, which is generally a difficult and time-consuming work. Based on the above explanation, the multipath and the transmission line approaches are both deterministic channel models. The two channel methods can only be applied to derive the communication channel response only when the topology of the network can be determined. But, for presenting the channel statistical properties, deterministic channel models are not appropriate. Hence, recently, statistical PLC channel modelling method has drawn considerable attention. This model, in theory, is necessary for determining the coverage, deployment and transmission capacity of powerline communication networks. It is obvious that the works on network coverage, channel coding and modulation techniques cannot be evaluated according to one or two specific network situations. Therefore, with an increase in demand for PLC technology, the statistical channel methods is necessary to determine how well PLC performs. PLC channel modelling comes with significant challenges.

The first challenge is from the transmission cable the electrical parameters. In transmission line theory, the cable is often evaluated using the lumped parameters resistance (R), capacitance (C), conductivity (G) and inductance (L) which should be reconsidered in the high frequency scenario. Usually, the R, C, G and L parameters are determined by the geometric structure of the cable, conductor and insulator materials. The cable types used in different papers, such as [35], [4] and [9], are from different countries, which means that it is difficult to compare the modelling results from different papers. Also it is difficult to verify the consistency of results of the modelling obtained from different methods. Therefore, getting a common cable parameters set to prove the consistency of results obtained from different modelling approaches is difficult to achieve. The other bottleneck is the topology. As stated above, the random topology variation across different homes and offices determines the channel statistical properties.

The PLC network topology will vary from one building to the next or from one place to another. For example, residential and office building topologies, or the topologies in Europe, Africa and South America will differ significantly. Hence, to determine the proper PLC channel topology for modelling purposes is a key issue to consider in PLC also. Generally, a tree structure [36] can be used to describe the topology of the powerline network. Therefore, the resultant statistical property of the PLC channel is determined from the results obtained from the random branch lengths, terminal loads and switching on/off of appliances. It is almost impossible to accurate determine this information of the PLC network in reality. For wireless communications research, there are some channel fading models which are commonly agreed upon, such as Nakagami, Rayleigh, Rician fading and Hata model for different terrains. Thus, we can directly compare research results obtained based on these channels with each other. By contrast, the channel modelling work done for powerline networks is in quite diverse settings. Thus, it is challenging task to obtain the detailed modelling information for the different scenarios and to verify the correctness of the results for each case.

CONCLUSION

In this paper, a comprehensive survey of PLC channel models has been presented. The challenges associated with PLC channel modeling are also discussed. PLC technology is promising in that the network infrastructure is already in place; but the channel characteristics are very dynamic and difficult to predict; hence PLC channel characterization and modelling continues to be an active research area.

International Journal of Engineering Research & Technology (IJERT)
ISSN: 2278-0181
Vol. 14 Issue 11 , November - 2025

REFERENCES

[1] J.O. Onunga and R.W Donaldson, "Personal computer communications on intra-building power line LANS using CSMA with priority acknowledgements," *IEEE Journal on Selected Areas in Communications*, vol. 7, no. 2, February 1989, pp. 180-191.

[2] L.T Berger, A. Schwager and J.J. Escudero-Garzas, "Power line communications for smart grid applications," *Journal of Electrical and Computer Engineering*, vol. 2013, Article 712376, 16 pages.

[3] H.C. Ferreira *et al.*, "Power Line Communications: An Overview," *IEEE AFRICON 1996*, 24-27 September 1996, Stellenbosch, South Africa, pp. 558-563.

[4] M. Zimmermann and K. Dostert, "A multi-path signal propagation model for the power line channel in the high frequency range," *Proceedings of the 3rd International Symposium on Power Line Communications and Applications*, Lancaster, U.K., 1999, pp. 45-51.

[5] H. Philipps, "Modeling of power line communications channels", *Proceedings of the 3rd International Symposium on Power Line Communications and Applications*, Lancaster, U.K., 1999, pp. 14-21.

[6] M. Zimmermann and K. Dostert, "A multipath model for the power line channel", *IEEE Transactions on Communications*, Vol. 50, No. 4, pp.553-559, April 2002.

[7] J. Anatory, M.M. Kissaka and N.H. Mvungi, "Channel model for broadband power line communication," *IEEE Transactions on Power Delivery*, vol. 22, no. 1, pp. 135-141, January 2007.

[8] A.M. Nyete, T. J. O. Afullo, and I.E. Davidson, "Statistical analysis and characterization of power line noise for telecommunication applications," *In Proceedings of the IEEE AFRICON 2015 Conference*, Addis Ababa, Ethiopia, 14–17 September 2015, pp. 213-217.

[9] H. Meng, S. Chen, Y.L. Guan, C. Law, P.L. So, E. Gunawan, T.T. Lie, "Modeling of Transfer Characteristics for the Broadband Power Line Communication Channel," IEEE Trans. Power Delivery, vol. 19, no. 3, pp. 1057-1064 July 2004.

[10] A.M. Nyete, T. J. O. Afullo, and I.E. Davidson, "On the application of non-parametric estimation methods for low voltage PLC network noise modelling," *In Proceedings of the Southern Africa Telecommunication Networks and Applications Conference (SATNAC)* 2015, Arabella Hotel & Spa, Western Cape, South Africa, 6-9 September 2015, pp. 59-63 .

[11] A.M. Nyete, T. J. O.Afullo, and I.E. Davidson, "Performance evaluation of an OFDM-based BPSK PLC system in an impulsive noise environment," *In PIERS Proceedings*, Guangzhou, China, August 25-28 2014, pp. 2510-2513.

[12] E. Biglieri, "coding and modulation for a horrible channel," *IEEE Communications Magazine*, May 2003, pp. 92-98.

[13] A.J. Han Vinck and J. Haring, "Coding and modulation for power-line communications," *ISPL2000*, pp. 265-272.

[14] A. M. Nyete, T. J. O. Afullo,, and I.E. Davidson, "Intra-building power network noise modelling in south africa," *In Proceedings of the 23rd Southern African Universities Power Engineering Conference*, University of Johannesburg, Johannesburg, South Africa, 28-30th January 2015, pp. 468-472.

[15] T.Q Bui, *Coded Modulation Techniques with Bit Interleaving and Iterative Processing for Impulsive Channels*, MSc. Thesis, University of Saskatchewan, 2006.

[16] A. Majumder and J. Caffrey, "Power line communications," *IEEE Potentials*, vol. 23, pp. 4-8, October 2004.

[17] T.S Pang, P.L So, K.Y See and A. Kamarul, "Common-mode current propagation in power line communication networks using multi-conductor transmission line theory," *In Proceedings of ISPLC2007*, 26-28 March 2007, pp. 517-522.

[18] M. Bogdanovic, " Computer based simulation model realization of OFDM communication over power lines," *In 20th Telecommunications Forum TELFOR 2012*, Serbia Belgrade, November 20-22, 2012, pp. 249-252.

[19] E.P Guillen, J.J Lopez and C.Y Barahoma, "Throughput analysis over power line communication channel in an electric noisy scenario," *World Academy of Science, Engineering and Technology*, vol. 19, pp. 206-212, 2012.

[20] G. Bumiller and N. Pirschel, "Airfield ground lighting automation system realized with power line communication," *In Proceedings of the ISPLC*, 2003, pp. 16-20.

[21] G. Griepentrog, "Powerline communication on 750V DC networks," *In Proceedings of the ISPLC*, 2001, pp. 259-265.

[22] J. Barnes, "A physical multi-path model for power distribution network propagation," *In Proceedings of the ISPLC*, Tokyo, Japan, March 1998, pp. 76-89.

[23] A. Dalby, "Signal transmission on powerlines-analysis of powerline circuits," *In Proceedings of the ISPLC*, Essen, Germany, 1-4, April 1997, pp. 37-44.

[24] O. Hooijen, "A channel model for the residential power circuit used as a digital communication medium," *IEEE Transactions on Electromagnetic Compatibility*, vol. 40, pp. 331-336, 1998.

[25] J. Anatory and N. Theethayi, *Broadband power line communication systems: Theory and Applications*, WitPress 2010.

[26] T. Esmailian, F. Kschischang and G. Gulak, "An in-building power line channel simulator," *In Proceedings of the ISPLC*, Greece, 2002, pp.1-5.

[27] M. Gotz, M. Rapp and K. Dostert, "Powerline channel characteristics and their effect on communication systems design," *IEEE Communications Magazine*, vol. 42, no. 4, pp. 78-86, April 2004.

[28] H. Philipps, "Performance measurements of powerline channels at high frequencies," *In Proceedings of the ISPLC, Tokyo, Japan, March 1998, pp. 229-237.*

[29] D.K. Cheng, *Fundamental of Engineering Electromagnetics*, Adison Wesley.

[30] D.M. Pozar, *Microwave Engineering*, New York: Wiley.

[31] G. Gonzalez, *Microwave Transistor Amplifiers*, Englewood Cliffs, NJ: Prentice Hall, 1997.

[32] J. Anatory *et. al.* "Broadband power-line communication channel model: Comparison between theory and experiments", Proc. IEEE Int. Symp. Power Line Communications and Its Applications, Jeju city, Jeju Island, pp.322 -324, Apr 2008.

[33] J. Anatory, N. Theethayi, R. Thottappillil, M.M. Kissaka and N.H. Mvungi, "The effects of load impedance, line length and branches in the BPLC- transmission lines analysis: a case of indoor voltage channel," *IEEE Transactions On Power Delivery,* vol.22, no 4, pp. 2150-2155, 2007.

[34] C.T Mulangu, *Channel Characterization for Broadband Power Line Communications*, PhD Thesis, University of KwaZulu-Natal, 2014.

[35] S. Galli and T. Banwell, "A novel approach to the modeling of the indoor power line channel-part ii: transfer function and its properties," IEEE Transactions on Power Delivery, vol. 20, pp. 1869– 1878, Jul. 2005.

[36] H. Hrasnica, A. Haidine, and R. Lehnert, "Broadband powerline communications networks-network design," John Wiley & Sons, Jun. 2004